Partitioning spectral absorption in case 2 waters: discrimination of dissolved and particulate components

Charles L. Gallegos and Patrick J. Neale

A series of three mathematical procedures is derived to discriminate the light absorption by phytoplankton, colored dissolved organic matter, and nonpigmented particulates in waters in which absorption is dominated by factors other than phytoplankton (i.e., case 2 waters). The procedures utilize normalized absorption cross-sectional spectra of the absorption components and matrix inversion to solve for the coefficients that scale the normalized spectra. The procedures differ in the amount of ancillary measurements incorporated to reduce the variability of the estimates. The procedure that incorporates no ancillary information is expected to be unbiased only over long time periods. Application of the procedures to a 15-day time series of continuously monitored data from the Rhode River, Maryland, revealed the presence of large (approximately twofold) changes in absorption at 440 nm over periods of a few hours. Hourly sampling over a 24-h period confirmed that the changes in measured optical coefficients corresponded to changes in water quality. Errors in estimates of absorption components were of a magnitude consistent with those observed in development of the procedures and confirmed the progressive improvement achieved by incorporation of additional information. Over the time period observed, changes in optical properties appeared to be driven by advective processes.

OCIS code: 010.4450.

1. Introduction

Remote sensing of surface ocean color has proven to be an extremely useful tool in ocean science, providing investigators with, among other things, mesoscale distributions of eddy fields and pigment biomass and estimates of regional[1] and even global primary production.[2] The interpretation of remotely sensed color has always depended on the ability to establish relationships between the contents of the water and its measurable optical properties. In particular, much research has been devoted to establishing relationships between the apparent optical properties, such as surface reflectance, which are measured by remote sensing instruments, and the inherent optical properties, which are determined solely by the kind and concentrations of dissolved and particulate matter in the water.[3]

Much of the emphasis to date has been on relatively clear oceanic waters, termed case 1 waters, which are those in which the optical properties are determined by water itself and by phytoplankton and their covarying degradation products.[4] Case 2 waters [i.e., those in which the optical properties are substantially affected by colored dissolved organic matter (CDOM) or suspended particulate matter from sources other than phytoplankton] comprise only approximately 2% of the world's oceanic and coastal waters, yet they are disproportionately important to human interests because of their general proximity to land and important function as fish nursery grounds and wildlife habitat.[4] In particular, communities of submerged vascular plants in shallow coastal waters are functionally important habitats that are especially sensitive to factors that result in reduced light availability.[5] Efforts to determine water quality requirements to protect these important habitats represent a point of interface between the environmental management and hydrologic optics communities.[6]

Recent developments in instrumentation for *in situ* measurement of spectral absorption and beam attenuation coefficients of water have afforded the opportunity to monitor or map the distribution of optical properties in considerable detail.[7–9] Interpretation of the measurements of optical properties in terms of

The authors are with the Smithsonian Environmental Research Center, P.O. Box 28, Edgewater, Maryland 21037. The e-mail address for C. L. Gallegos is gallegos@serc.si.edu.

Received 14 December 2001; revised manuscript received 29 April 2002.

0003-6935/02/214220-14$15.00/0

temporal variability or spatial fields of the causative factors presupposes a model for the analysis of observed spectra. Such models have been proposed[10] and applied in various regions, both in under-way transects[9] and with moored instruments.[8]

The model of Roesler *et al.*[10] does not attempt to distinguish absorption by CDOM from that by nonpigmented particulates because of the similarity in their spectral shapes. In applying the model of Roesler *et al.*[10] to absorption and attenuation data monitored *in situ*, Chang and Dickey[8] used direct measurements of CDOM absorption from bottle casts that coincided in location and time with *in situ* measurements to differentiate dissolved from particulate absorption in the coinciding *in situ* measurements. Such ancillary measurements, when available, greatly improve the confidence with which we can extract the components of absorption from measurements of total absorption. With *in situ* monitoring or under-way mapping, however, we can expect that ancillary measurements will be available only for a minor proportion of measurements.

Here we present a suite of procedures for estimating components of absorption that vary depending on the availability of ancillary measurements. Emphasis is placed on discriminating absorption by CDOM from that by nonalgal particulate matter. We evaluate the procedures using measurements of absorption and scattering coefficients in discrete water samples from contrasting case 2 waters—the turbidity-dominated Rhode River, Maryland, and the CDOM-dominated St. Johns River, Florida. We demonstrate applicability of the procedures using data from continuous monitoring in the Rhode River.

2. Analysis of Absorption Spectra

Absorption is an inherent optical property[11] and therefore can be expressed as the sum of contributions by individual components, that is, by water and all absorbing dissolved and particulate matter in the sample. Thus we can express the total absorption coefficient $a_t(\lambda)$ as

$$a_t(\lambda) = a_w(\lambda) + a_g(\lambda) + a_p(\lambda), \tag{1}$$

where a_w is absorption by water, a_g is absorption by CDOM (i.e. gelbstoff), $a_p(\lambda)$ is absorption by particulate matter, and all are functions of the wavelength of light λ. Absorption by particulate matter can be represented by the sum of absorption that is due to *in vivo* phytoplankton pigments $a_\phi(\lambda)$ and that by all remaining particulate matter $a_{p-\phi}(\lambda)$.[12] Operationally, $a_{p-\phi}(\lambda)$ includes absorption by nonpigmented cellular material of living phytoplankton and heterotrophic plankton, plant and animal detritus, and mineral particles. We comment on prospects for further separation of $a_{p-\phi}(\lambda)$ into contributions by mineral and organic fractions in Section 6.

Field measurements of total absorption and beam attenuation can be made with a flow-through absorption–attenuation meter (e.g., WET Labs ac-9). The instruments are calibrated to optically pure water, and thus the absorption and attenuation coefficient of pure water are not included in the sample measurements, yielding $a_{t-w}(\lambda)$ and $c_{t-w}(\lambda)$. However, the reflective tube absorption–attenuation meter overestimates $a_{t-w}(\lambda)$, which is due to loss of photons that are not detected because of backscattering within the reflective tube.[13] Various corrections have been suggested,[14] including subtraction of $a(715)$ from all other wavelengths[8,9] and subtraction of a percentage of measured spectral scattering.[15] Kirk,[13] using Monte Carlo modeling of radiative transport within the reflective tube absorption meter, demonstrated that the error was proportional to the total scattering coefficient b ($=c - a$). That is,

$$a_{t-w}(\lambda) = a_m(\lambda) - wb(\lambda), \tag{2}$$

where $a_m(\lambda)$ are the temperature- and salinity- (and drift-, if necessary) corrected absorption coefficients actually measured by the ac-9, and w is a coefficient that depends on the shape of the volume scattering function and optical characteristics of the instrument (e.g., acceptance angle of detector, path length, reflectivity of the tube). Equation (2) is not immediately applicable to ac-9 measurements because the scattering coefficients calculated from ac-9 measurements are underestimates of the true $b(\lambda)$ for the same reasons that $a_m(\lambda)$ overestimate $a_{t-w}(\lambda)$. We can, however, accomplish the same correction as Eq. (2) by applying a slightly larger correction factor ϵ to the measured scattering coefficients. Let $b_m(\lambda) = c_{t-w}(\lambda) - a_m(\lambda)$ denote scattering coefficients calculated from quantities directly measured by the ac-9; then it can be shown that

$$a_{t-w}(\lambda) = a_m(\lambda) - \epsilon b_m(\lambda), \tag{3}$$

where ϵ is related to w by the identity $\epsilon = w/(1 - w)$. ϵ is estimated from the data by a procedure, described below, that allows for residual absorption by CDOM or by particulate matter in the near infrared in case 2 waters.

The equation for extraction of absorption components from ac-9 measurements can now be written:

$$a_m(\lambda) = a_g(\lambda) + a_\phi(\lambda) + a_{p-\phi}(\lambda) + \epsilon b_m(\lambda). \tag{4}$$

We now define normalized absorption spectra for each of the components:

$$g(\lambda) = \frac{a_g(\lambda)}{a_g(440)}, \tag{5a}$$

$$\phi(\lambda) = \frac{a_\phi(\lambda)}{a_\phi(676)}, \tag{5b}$$

$$p(\lambda) = \frac{a_{p-\phi}(\lambda)}{a_{p-\phi}(440)}, \tag{5c}$$

where $g(\lambda)$, $\phi(\lambda)$, and $p(\lambda)$ are, respectively, the normalized absorption spectra for CDOM, phytoplankton pigment, and nonpigmented particulates. We chose 440 nm as a reference wavelength for absorption by CDOM and nonpigmented particulates by

convention,[16] and 676 nm was chosen to normalize $a_\phi(\lambda)$ because it is the location of an absorption peak for phytoplankton chlorophyll that is readily distinguished from CDOM and other particulate matter.

A. Unconstrained Procedure

Assuming that mean spectral values for the normalized absorption spectra can be determined for a region of interest, then the characteristic absorption coefficients at the appropriate reference wavelengths can be determined when we solve the system

$$\mathbf{a}_0 = \mathbf{N}_0^{-1}\mathbf{a}_m, \tag{6}$$

where $\mathbf{a}_0$ is the vector of coefficients to be estimated $[a_g(440), a_\phi(676), a_{p-\phi}(440), \epsilon]^T$, $\mathbf{a}_m$ is the vector of absorption coefficients measured by the ac-9 $[a_m(\lambda_1), \ldots, a_m(\lambda_4)]^T$, and $\mathbf{N}_0$ is the matrix of coefficients

$$\mathbf{N}_0 = \begin{bmatrix} g(\lambda_1) & \phi(\lambda_1) & p(\lambda_1) & b_m(\lambda_1) \\ \cdot & & & \cdot \\ \cdot & & & \cdot \\ g(\lambda_4) & \phi(\lambda_4) & p(\lambda_4) & b_m(\lambda_4) \end{bmatrix}. \tag{7}$$

If the normalized absorption spectra were invariant and perfectly known and if $a_m(\lambda)$ were error free, the choice of wavelengths in Eq. (7) would not matter. However, because of expected levels of uncertainties, we choose wavelengths to maximize the information about the unknown absorption coefficients. We routinely use $\lambda_1 = 412$ nm because it is a maximum (among the wavelengths available with the ac-9) for absorption by CDOM; $\lambda_2 = 488$ nm because it is the wavelength at which $g(\lambda)$, $\phi(\lambda)$, and $p(\lambda)$ have their maximum separation; $\lambda_3 = 676$ nm because it is an absorption peak for $\phi(\lambda)$; and $\lambda_4 = 715$ nm because $a_m(715)$ is governed largely by ϵ. This procedure makes no assumptions regarding negligible absorption by CDOM or by tripton at either 676 or 715 nm.[17] Furthermore, Eqs. (6) and (7) neither require nor utilize any supporting measurements that may be available. We call this the unconstrained procedure.

B. Statistically Augmented Procedure

In many coastal regions, normalized absorption spectra for CDOM and nonalgal particulates are similar, both conforming to negative exponential functions of wavelength with similar spectral slopes.[10,18–20] Consequently, previous attempts to partition absorption spectra have generally combined absorption by CDOM and by nonalgal particulates into a single term[9,10] or used direct measurements of $a_g(\lambda)$ to achieve the decomposition.[8] Anticipating the difficulty of distinguishing a_g from $a_{p-\phi}$, we introduce two modifications of Eqs. (6) and (7) that make use of successively more ancillary measurements.

Noting that scattering by particulate matter far exceeds that by dissolved matter or by water itself,[16] we suppose that the scattering coefficient might give an indication of the magnitude of $a_{p-\phi}(440)$, i.e.,

$$a_{p-\phi}(440) = \rho b(440) = \rho b_m(440)(1 + \epsilon), \tag{8}$$

where ρ is the absorption-to-scattering ratio at 440 nm and is related to the particle scattering albedo[21] ω_p by $\rho = (1 - \omega_p)/\omega_p$. The value of ρ, for which we present a site-specific statistical model, is expected to vary with the size and composition of the particulate matter. Substituting Eq. (8) into Eq. (4) and solving as before, we obtain

$$\mathbf{a}_1 = \mathbf{N}_1^{-1}\mathbf{a}_{m-p}, \tag{9}$$

where $\mathbf{a}_1$ is the vector of coefficients to be estimated $[a_g(440), a_\phi(676), \epsilon]^T$, $\mathbf{a}_{m-p}$ is the vector of modified measured absorption coefficients $[a_m(\lambda_1) - \rho b_m(440)p(\lambda_1), \ldots, a_m(\lambda_3) - \rho b_m(440)p(\lambda_3)]^T$, and $\mathbf{N}_1$ is the 3×3 matrix of coefficients

$$\mathbf{N}_1 = \begin{bmatrix} g(\lambda_1) & \phi(\lambda_1) & b_m(\lambda_1) + \rho b_m(440)p(\lambda_1) \\ \cdots & \cdots & \cdots \\ g(\lambda_3) & \phi(\lambda_3) & b_m(\lambda_3) + \rho b_m(440)p(\lambda_3) \end{bmatrix}. \tag{10}$$

We refer to Eqs. (8)–(10) as the statistically augmented procedure because it uses a site-specific, statistically derived estimate of the absorption-to-scattering ratio to help distinguish between absorption by dissolved matter and nonalgal particulates. We use measurements on discrete water samples to estimate normalized absorption spectra and to develop a statistical model for ρ.

C. Measurement-Constrained Procedure

Finally, if measurements of absorption by CDOM are available and we wish to use them to constrain the other estimated quantities, we can write the system

$$\mathbf{a}_2 = \mathbf{N}_2^{-1} \cdot \mathbf{a}_{m-g}, \tag{11}$$

where $\mathbf{a}_2$ is the vector of unknowns $[a_\phi(676), a_{p-\phi}(440), \epsilon]^T$, $\mathbf{a}_{m-g} = [a_m(\lambda_1) - a_g(440)g(\lambda_1), \ldots, a_m(\lambda_3) - a_g(440)g(\lambda_3)]^T$, and $\mathbf{N}_2$ is a 3×3 matrix identical to $\mathbf{N}_0$, omitting the column for $g(\lambda)$ and the row for λ_2 (488 nm). We refer to Eq. (11) as the measurement-constrained procedure because measurements of absorption by CDOM are specified exactly. This procedure would be appropriate if two ac-9s were operated in parallel with one instrument having a 0.2-μm filter placed on the intake port (in waters where this can be done without rapid clogging of the filter), thereby providing simultaneous estimates of $a_g(\lambda)$.

3. Study Sites

A. Rhode River

The Rhode River in Maryland is a small tributary embayment on the western shore of the mesohaline reach of the Chesapeake Bay. The system is shallow (mean depth 2 m, maximum depth 4 m), turbid,[20] and eutrophic[22,23] (mean summer chlorophyll concentration is 20–40 mg m^{-3}). Salinity varies seasonally

and spatially from 0 to 14 practical salinity units (psu) at the upstream stations and from approximately 2 to 20 psu at the mouth, depending on flow of the Susquehanna River, the main freshwater source to the upper Chesapeake Bay.[24] The mean tidal range is 30 cm, but wind and barometric pressure gradients frequently cause much larger changes in water level. Samples for measurement of optical properties in the Rhode River (n = 135) were collected approximately weekly from January 1999 through May 2000. Three stations were occupied, ranging from its mouth (approximately 3.5 m deep) where it intersects the Chesapeake Bay, a station off the Smithsonian pier (approximately 1.7 m deep), and in a shallow (approximately 1 m deep) region of subtidal mudflats just downstream of the divergence of Muddy Creek, the main freshwater source to the Rhode River (see Ref. 24).

B. St. Johns River

The St. Johns River is a shallow blackwater estuary on the northeast coast of Florida. Average depth in the northern 150-km stretch sampled here is approximately 3 m, with a maximum of 24 m. Average tidal amplitude is 1.38 m at the ocean inlet and varies unevenly upstream in relation to channel morphology and other factors.[25] The river has its source in the floodplains north of Lake Okeechobee. These floodplains and other wetlands are the source of high concentrations of CDOM, which generally peak after sustained rains or short-term flood events that result in fresh inputs from the wetlands. Salinity distributions are vertically homogeneous.[25] In this study, we occupied stations at the seaward boundary, within the mixing zone (two stations, salinity 5–30 psu), and in the tidal fresh ranges (five stations, salinity <1 psu). Samples from the St. Johns River were collected quarterly from August 1999 to October 2000.

4. Materials and Methods

A. Laboratory Measurements

Samples from stations in the Rhode River, Maryland, and St. Johns River, Florida, were collected with a 2-l Labline Teflon sampler that was slowly lowered and raised over the depth of the water column (1–3 m) to collect a vertically integrated sample. Water samples were transported to the laboratory where we measured optical properties and water quality parameters, i.e., turbidity and chlorophyll concentration. In the laboratory we measured spectral absorption [$a_m(\lambda)$] and beam attenuation [$c_{t-w}(\lambda)$] coefficients at nine wavelengths (412, 440, 488, 510, 532, 555, 650, 676, and 715 nm) using a flow-through absorption–attenuation meter (ac-9, WET Labs). Water was gravity fed through the instrument at a flow rate of approximately 1.5 l min^{-1}, and data were logged with the manufacturer's Wetview software. Temperature- and salinity-corrected absorption coefficients were corrected for backscatter[13,14] as described below.

We measured absorption by CDOM on water filtered through a 0.2-μm-pore-diameter polycarbonate membrane filter (Poretics) using 5-cm path-length quartz cells in a Cary-4 dual-beam spectrophotometer with an accuracy better than 0.01 absorption unit. We converted measurements in absorption units to *in situ* absorption coefficients $a_g(\lambda)$ by multiplying by 2.303 [i.e., ln(10)] and dividing by the path length 0.05 m.

We measured absorption by particulate matter $a_p(\lambda)$ using the quantitative filter pad technique.[26] A volume of water was filtered onto a 25-mm glass fiber filter (GF/F, Whatman), and it was frozen (−20 °C) for <4 weeks. For measurements, the filters were thawed and rewetted with 200 μl of filtered distilled water and placed next to the exit window of the sample beam of the Cary spectrophotometer. Absorbance was measured relative to a moistened blank GF/F placed next to the exit window of the reference beam. Filters were then extracted in methanol for 4 h to remove phytoplankton pigments[26]; they were then rewetted and scanned again. An average of five absorbance readings from 746 to 750 nm was subtracted from the extracted readings as a baseline correction. This correction was not needed for preextracted measurements. Measured particulate absorbances [$a_p'(\lambda)$] were converted into *in situ* particulate absorption coefficients [$a_p(\lambda)$] following the methods presented in Kishino *et al.*[26] Procedures to estimate the path-length amplification factor β are described in Subsection 4.C. The potential exists with this procedure to underestimate absorption by particulate matter with a size less than approximately 0.7 μm, the nominal pore size of GF/Fs. We expect this error to be small in these waters, where filters clog quickly, reducing the effective pore size of GF/Fs.

For determination of chlorophyll concentrations, whole-water samples were filtered onto GF/Fs and stored frozen up to 4 weeks. Filters were thawed and extracted overnight at 4 °C in the dark. Chlorophyll concentrations, uncorrected for phaeopigments, were calculated from spectrophotometric absorbance measurements by the equations of Jeffrey and Humphrey.[27] Turbidity in nephelometric turbidity units was measured with a Hach 2100N turbidimeter.

B. Optical Monitoring

An ac-9 unit for continuous monitoring was housed in a monitoring shed at the end of the Smithsonian pier on the Rhode River. Flow to the ac-9 was by gravity feed. Water from the estuary was pumped into an open-topped polyvinyl chloride cylinder with a return arm to provide a constant head. A spigot and tubing located near the bottom of the cylinder conducted water past a bubble-trap standpipe to the ac-9. A WET Labs MPak was used to control the ac-9 and log the data. Once per hour the ac-9 was turned on, allowed to warm up for 5 min, and sampled for 1 min at 6 Hz.

To reduce fouling within the cylinder, the pump was operated only 15 min/h, extending from approx-

imately 10 min before to 5 min after sampling by the ac-9. At the conclusion of a sampling cycle, a solenoid valve was opened that allowed approximately 60 ml of bromide solution to flow through the standpipe and ac-9 to inhibit growth of fouling organisms on the optical surfaces of the ac-9. Timing of the pump and solenoid valve was controlled by a Campbell Scientific CR10 data logger and control module. This procedure flushed the system with bromide, but did not leave bromide standing in the tubes between measurements. Therefore we detected no effect of the bromide on measured absorption and attenuation coefficients.

Data were downloaded, and the ac-9 was cleaned three times per week. Cleaning was commenced immediately following a reading. Water from that reading was collected and run through the meter again after cleaning to correct for drift that was due to accumulation of particulate matter during the previous monitoring period. Cleaning and downloading generally took less than 1 h, so that hourly sampling was usually not interrupted.

We calculated the change in absorption and beam attenuation coefficients after cleaning and applied the difference incrementally over the time period since the last cleaning, which was generally <3 days. The change in the reading after cleaning was generally approximately -13% for $a(\lambda)$ and -7% for $c_{t-w}(\lambda)$. Temperature and salinity at the site were monitored at hourly intervals coinciding with ac-9 measurements by a Hydrolab minisonde. Corrections for the temperature and salinity dependence of the absorption coefficient of pure water were applied according to the manufacturer's specifications. In these waters, the resulting corrections were always small in relation to the overall magnitude and relative variability in measured optical coefficients.

C. Calculation of ϵ, β, and ρ

Laboratory estimates of optical properties on profile water samples consist of $a_m(\lambda)$ measured with the ac-9, $a_g(\lambda)$ measured spectrophotometrically on 0.2-μm filtered water, and $a_p'(\lambda) = \beta a_p(\lambda)$ by the quantitative filter technique. For these water samples, we calculated ϵ and β by assuming that, when appropriate corrections are applied, the ac-9 will give estimates of absorption consistent with the sum of laboratory measurements of $a_g(\lambda)$ and $a_p'(\lambda)/\beta$. That is,

$$a_m(\lambda) - \epsilon b_m(\lambda) = a_g(\lambda) + \frac{1}{\beta} a_p'(\lambda). \qquad (12)$$

We solve Eq. (12) for ϵ and β using observations at two wavelengths, 440 and 715 nm. With these estimates of ϵ and β, we then estimated ρ for discrete water samples by

$$\rho = \frac{a_{p-\phi}'(440)}{\beta b_m(440)(1+\epsilon)}, \qquad (13)$$

where $a_{p-\phi}'(440)$ is the measured absorption coefficient at 440 nm of the depigmented filter pad.

For estimation of normalized absorption spectra [Eqs. (5a)–(5c)] and development of the statistically augmented procedure [Eqs. (8)–(10)], we randomly assigned each set of measurements to either a development set (two thirds) or an evaluation set (one third). We also used measurements in the development set to estimate ϵ, β, and ρ by Eqs. (12) and (13). Note that these estimates of ϵ, which used both ac-9 measurements of absorption and attenuation and laboratory measurements of dissolved and particulate absorption, differ from those determined by solution of Eqs. (6), (9), or (11), which use only ac-9 measurements. Those estimated from Eq. (12) were used with the development data set for estimation of a statistical model for ρ and are referred to as measured ϵ in comparisons with those ϵ calculated by Eq. (6), (9), or (11) with the evaluation set.

We developed a site-specific statistical model for ρ by reasoning that the underlying correlations in the data produced by variability in ρ should result in subtle but detectable changes in the shape of the absorption (and perhaps also the scattering) spectra. We performed a principal components analysis on measured absorption spectra normalized to $a_m(412)$ and scattering spectra normalized to $b_m(412)$. Values of ρ estimated by Eq. (13) were regressed against principal component scores, as well as scaling coefficients $a_m(412)$ and $b_m(412)$ for estimation of the site-specific statistical model.

5. Results

A. Coefficients Estimated from Laboratory Measurements

Values of the parameters that we calculated using Eqs. (12) and (13) were within the expected ranges (Table 1), with the exception of several samples from both locations in which calculated $\beta < 1$, which is theoretically impossible. Such a result is easily understood as an overestimate of $a_m(\lambda)$, for example, because of inadequately cleaned surfaces in the ac-9. We excluded those samples from the analysis for estimating a statistical model for ρ because an underestimate of β translates directly to an overestimate of ρ [Eq. (13)]. Estimates of particle scattering albedo calculated from ρ ranged from 0.8, approximately the minimum for phytoplankton, to 0.96, characteristic of strongly scattering mineral particulates.[21,28] Mean values for ϵ estimated from laboratory measurements (Table 1) were typical of those expected for particulate matter dominated by inorganic solids.[13]

Principal components analysis of normalized absorption and scattering spectra indicated that spectral shapes were relatively conservative. In the Rhode River, the first principal component explained 78% of the variance in the normalized a_m spectra, with the elements of the eigenvector varying only weakly with wavelength (Fig. 1). The second principal component explained 14.5% of the variance and appeared to accentuate covarying chlorophyll and (dissolved or particulate) nonpigmented absorption,

Table 1. Statistics of Parameter Values Estimated from Laboratory Measurements of Inherent Optical Properties with Eqs. (12) and (13)

Parameter	Rhode River, n = 109 (94)[a]				St. Johns River, n = 31 (23)			
	Mean	Minimum	Maximum	Coefficient of Variation	Mean	Minimum	Maximum	Coefficient Value
β	1.52	0.58	5.72	0.44	1.30	0.47	3.97	0.49
	(1.65)	(1.07)	(5.72)	(0.40)	(1.47)	(1.05)	(3.97)	(0.44)
ϵ	0.184	0.079	0.331	0.24	0.212	0.077	0.564	0.40
	(0.189)	(0.079)	(0.331)	(0.20)	(0.214)	(0.119)	(0.564)	(0.40)
ρ	0.116	0.042	0.263	0.42	0.157	0.051	0.571	0.68
	(0.105)	(0.042)	(0.263)	(0.33)	(0.124)	(0.051)	(0.264)	(0.43)

[a]Values in parentheses are statistics recalculated omitting samples for which calculated $\beta < 1$.

but did not enter significantly into the regression for ρ. The third principal component, although only explaining 4% of the variance, entered significantly into the regression for ρ and had eigenvectors that appeared to vary with the ratio $a_\phi(676):a_\phi(440)$. Only the first principal component of the normalized scattering coefficients entered significantly into the regression for ρ, and the eigenvectors varied with wavelength in a manner similar to those for the first eigenvector of normalized absorption spectra (Fig. 1).

A linear regression of ρ against the significant principal component scores for normalized $a_m(\lambda)$ and $b_m(\lambda)$ along with the scaling coefficients $a_m(412)$ and $b(412)$ explained 68% of the variance in measured ρ. Inclusion of the scaling coefficients $a_m(412)$ and $b_m(412)$ in the regression for ρ indicates that spectral shape alone is insufficient to infer the value of ρ and that overall magnitude of absorption and scattering are important as well. The sign of the partial coefficients for $a_m(412)$ and $b_m(412)$ were as expected, i.e., positive for $a_m(412)$ and negative for $b_m(412)$.

In the St. Johns River, no significant regression was found between ρ and principal component scores of the normalized a_m and b_m spectra. Therefore we used the average value of ρ (Table 1) as determined by Eq. (13) for the statistically augmented procedure for that system.

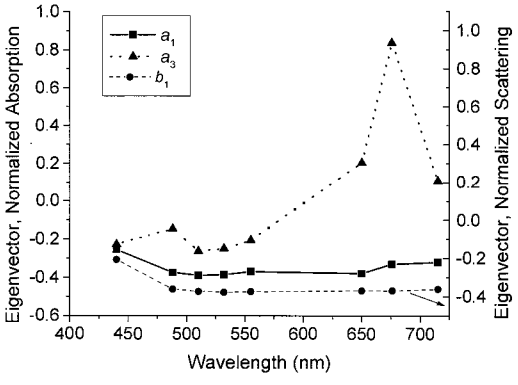

Fig. 1. Eigenvectors of the principal components of normalized absorption and scattering spectra that entered significantly into the linear regression for the absorption-to-scattering ratio ρ for data from the Rhode River. First (squares) and third (triangles) principal components for absorption (left y axis) and the first (circles) principal component for scattering (right y axis) entered the regression for ρ.

B. Normalized Absorption Spectra

The shapes of the normalized absorption spectra for the Rhode River were similar to those from the St. Johns River (Fig. 2), although differences in numerical values could be discerned (Table 2). The spectral shape of absorption by CDOM, which generally conforms to a negative exponential function of wavelength, has been well characterized in a variety of environments.[29,30] The coefficients determined on the development data set in the Rhode River (Table 2) were determined from a negative exponential with a spectral slope of 0.018 nm^{-1} whereas those from the St. Johns River were fit with a spectral slope of 0.015 nm^{-1}.

The absorption spectrum by phytoplankton has also been well studied. It has been frequently reported that the chlorophyll-specific absorption $a_\phi^*(\lambda) \equiv a_\phi(\lambda)/[\mathrm{Chl}]$ where [Chl] is the concentration of chlorophyll, declines with increasing [Chl].[9,31] This has been ascribed to self-shading (package) effects in oceanic phytoplankton acclimated to low-light availability. However, the chlorophyll concentration dependence was not found to be applicable in these waters where the optical properties are often only weakly dependent on phytoplankton chlorophyll. We would expect that cellular chlorophyll packaging might be uncoupled from chlorophyll concentration in case 2 waters because overall optical properties and hence mean light availability in the water column depend on factors other than [Chl]. Our values for $\phi(\lambda)$ (Table 2), determined as averages of $a_\phi(\lambda)/a_\phi(676)$ from filter pad measurements, showed no systematic dependence on [Chl]. The relative magnitude of the error bars (±2 standard errors) was greater for absorption by phytoplankton than for either of the other components (Fig. 2).

Absorption spectra by nonalgal particulates have been reported to be variously shaped, with most resembling a negative exponential[10,18,20] or U shaped.[32,33] Our average spectrum for $p(\lambda)$ (Table 2) strongly resembled a negative exponential, although not perfectly so. For that reason, values reported in Table 2 and that are used in Eqs. (7) and (10) were determined as averages of $a_{p-\phi}(\lambda)/a_{p-\phi}(440)$ mea-

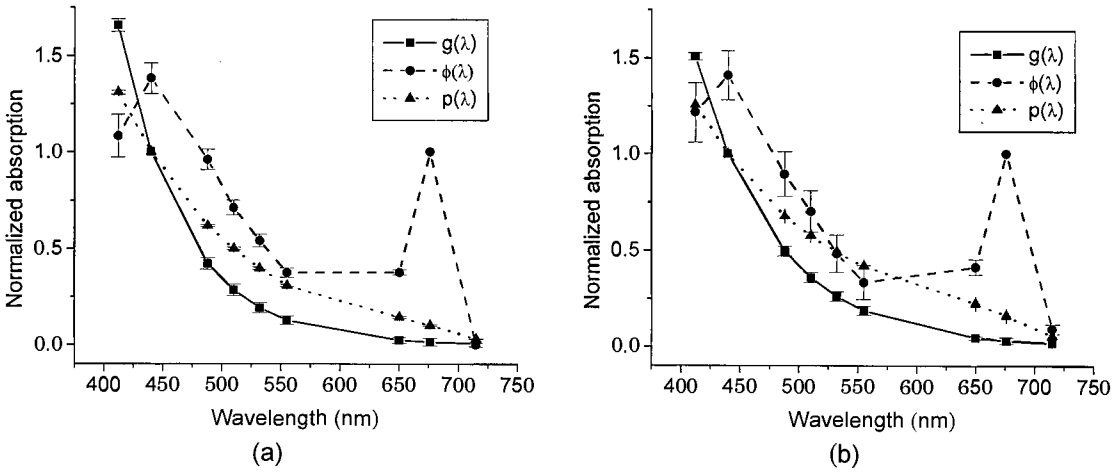

Fig. 2. Average absorption spectra normalized to absorption at a reference wavelength for (squares) CDOM [$g(\lambda)$], (circles) phytoplankton pigment [$\phi(\lambda)$], and (triangles) nonpigmented particulate matter [$p(\lambda)$]: (a) Rhode River, Maryland; (b) St. Johns River, Florida. Error bars are ±2 standard errors.

sured on depigmented filter pads—i.e., no function was fit to $p(\lambda)$. In general, the procedures in Eqs. (6)–(11) can accommodate arbitrarily shaped normalized absorption spectra for any of the components, provided that they faithfully represent the actual shape.

C. Application to Discrete Water Samples

Estimates of the backscatter correction factor ϵ when all three procedures are used were highly correlated with those calculated from measurements both in the Rhode River [Fig. 3(a)] and in the St. Johns River [Fig. 4(a)]. Interestingly, correlations between measured and estimated ϵ made by the measurement-constrained solution were lowest of the three procedures in the Rhode River and highest in the St. Johns River (Table 3). This result corresponds with the observation that absorption by CDOM is generally the lowest component in the Rhode River, whereas CDOM absorption is the dominant component in the St. Johns River. Although estimates of ϵ were biased slightly high in the Rhode River and slightly low in the St. Johns River, mean residuals were generally low and a small (≤5%) fraction of typical values.

Table 2. Normalized Absorption Coefficients for Absorption by CDOM [$g(\lambda)$], Phytoplankton Pigments [$\phi(\lambda)$], and All Other Particulates [$p(\lambda)$]

	Rhode River			St. Johns River		
Wavelength	$g(\lambda)$	$\phi(\lambda)$	$p(\lambda)$	$g(\lambda)$	$\phi(\lambda)$	$p(\lambda)$
412	1.655	1.083	1.310	1.590	1.252	1.255
440	1.000	1.383	1.000	1.000	1.423	1.000
488	0.421	0.961	0.618	0.515	0.902	0.677
512	0.284	0.712	0.499	0.396	0.700	0.576
532	0.191	0.541	0.397	0.303	0.482	0.491
555	0.126	0.374	0.306	0.228	0.331	0.419
650	0.023	0.376	0.143	0.057	0.397	0.222
676	0.014	1.000	0.100	0.044	1.000	0.161
715	0.007	0.000	0.030	0.000	0.086	0.054

Estimates of $a_g(440)$ with the unconstrained solution procedure on data from the Rhode River were unbiased but had poor correspondence with measured values [Table 3; Fig. 3(b), filled squares]. The statistically augmented solution [Eqs. (8)–(10)] improved the correlations between calculated and measured $a_g(440)$ in the Rhode River, although estimates by that procedure were biased slightly high (0.13 m^{-1}, Table 3). Estimates of $a_g(440)$ made with the unconstrained procedure with data from the St. Johns River were better correlated with measurements than in the Rhode River (Table 3), although the magnitudes of errors were larger there because of the much larger overall range of measured values. Estimation of $a_g(440)$ by the statistically augmented procedure in the St. Johns River improved the r^2 to 0.84 (Table 3). In the St. Johns River there were several samples in which $c_{t-w}(412)$ exceeded 30 m^{-1} [Figs. 4(b)–4(d), triangles], which may exceed the reliable operating range of the instrument. We omitted these samples from the statistical evaluation. We also note that, in the comparisons between measured and estimated quantities in Figs. 3–4, only measured and estimated $a_g(440)$ are truly independent because the procedure to calculate measured ϵ, $a_\phi(676)$, and $a_{p-\phi}(440)$ employed ac-9 measurements in the calculation of β.

Calculated values of $a_\phi(676)$ explained approximately 70–80% of the variance in measurements by all solution procedures in the Rhode River (Table 3). For the particulate components, there is error in both the estimated value and the measured value because of the uncertainty in β. Estimates were negatively biased when all three calculation procedures were used in the Rhode River [Table 3, Fig. 3(c)]. The systematic underestimates occurred primarily in the middle of the observed range, between approximately 0.5 and 1.25 m^{-1} [Fig. 3(c)]. The St. Johns River estimates of $a_\phi(676)$ made with the unconstrained and statistically augmented procedures were unbi-

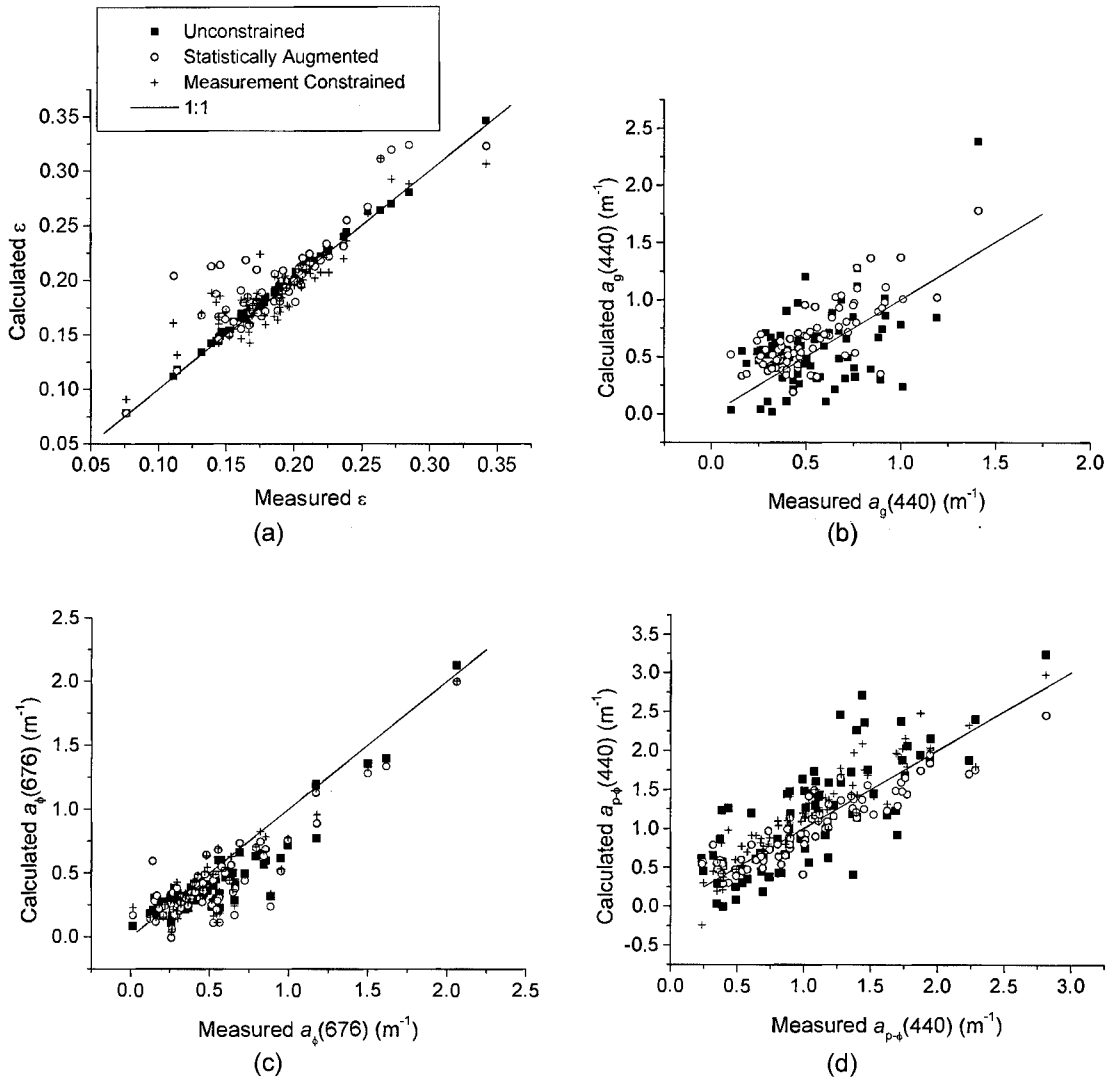

Fig. 3. Comparison of optical parameters calculated by the three solution with measurements made in the laboratory for Rhode River, Maryland: (a) backscatter correction factor ϵ; (b) absorption by CDOM at 440 nm, $a_g(440)$; (c) absorption by phytoplankton pigment at 676 nm, $a_\phi(676)$; (d) absorption by nonpigmented particulates at 440 nm, $a_{p-\phi}(440)$.

ased and correlated with measurements, more strongly so for the unconstrained than for the statistically augmented procedure [Table 3, Fig. 4(c)]. The measurement-constrained calculations of $a_\phi(676)$ in the St. Johns River were uncorrelated with measurements and were negatively biased (Table 3).

Estimates of absorption by nonalgal particulate matter $a_{p-\phi}(440)$ made with the unconstrained procedure in the Rhode River were unbiased with respect to measurements [Table 3, Fig. 3(d)]. The correlation between estimated and observed was higher when the statistically augmented procedure was used although estimates were biased slightly low (-0.05 m^{-1}, Table 3). Estimates made with the measurement-constrained procedure were positively biased (Table 3). In the St. Johns River, accurate estimates of $a_{p-\phi}(440)$ could not be determined by either the unconstrained or by the measurement-constrained procedures [Table 3, Fig. 4(d)]. Estimates in the St. Johns River with the statistically augmented procedure were unbiased and better correlated with measurements ($r^2 = 0.46$) than those made with the other procedures (Table 3).

D. *In Situ* Monitoring

A 15-day time series of measurements (with one 18-h gap that was due to a recorder failure) from late February to early March 2000 is illustrated in Fig. 5. Raw measurements at 440 nm prior to any correction ranged from 2 to 8 m^{-1} and were characterized by many abrupt and short-term changes [Fig. 5(a), solid curve]. Corrections for temperature and salinity (not shown) ranged from -0.05 m^{-1} at 715 nm to $+0.002$ m^{-1} at 412 nm. Subtractions for drift, shown in Fig. 5(a) as vertical dashed curves were larger, ranging from 0.5 to 1.5 m^{-1} at 440 nm. The correction for drift removed the abrupt declines asso-

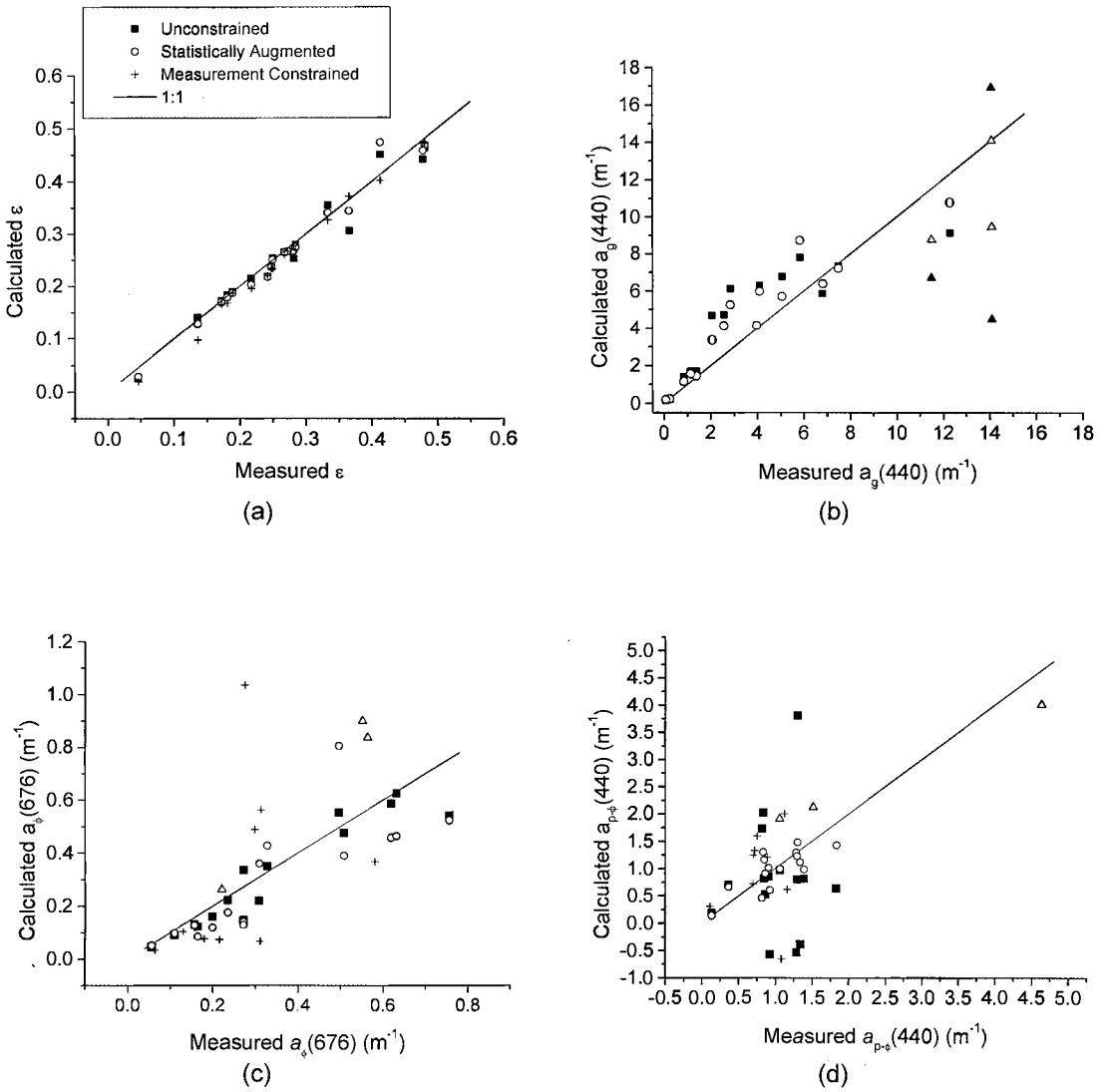

Fig. 4. As in Fig. 3, but for the St. Johns River, Florida. Triangles denote measurements omitted from statistical evaluation (see text): solid triangles, estimated by unconstrained procedure; open triangles, estimated by statistically augmented procedure.

ciated with cleaning of the instrument [Fig. 5(a), dashed curves; vertical dashed curves mark times of cleaning), but left the large spikes relatively unaltered. Corrections for backscatter made the largest changes in recorded values, reducing the overall mean of the series from 3.5 m^{-1} (drift corrected) to 1.7 m^{-1} [Fig. 5(a), dotted curves]. The relative magnitude of the short-term variability was reduced somewhat by backscatter correction, but several pronounced spikes remain.

Application of the unconstrained solution to estimate components of absorption at 440 nm [Fig. 5(b)] gave results commensurate with those based on profile samples. That is, nonpigmented particulates clearly dominated the total absorption at 440 nm in the Rhode River; and absorption by phytoplankton and by CDOM were of fairly similar magnitude, shifting from slightly higher a_ϕ at the beginning to slightly higher a_g near the end of the record [Fig. 5(b)]. Note that phytoplankton absorption in Fig. 5(b) is reported for 440 nm [i.e., $\phi(440)a_\phi(676)$] to maintain additivity of the absorption components.

We collected water from the outflow of the ac-9 at hourly intervals for 24 h on 7–8 March 2000 to determine if the short-term variability in the recorded data represented actual changes in standard water quality measurements (e.g., turbidity, chlorophyll) and to further test the performance of solutions with continuously monitored data. Scattering coefficient at 440 nm was larger than but closely paralleled changes in measured turbidity [Fig. 6(a)]. Times of peak scattering coefficient seemed to correspond with times of high water level [Fig. 6(a), thin curve], indicating that the changes are likely related to passage of tidal fronts.

The unconstrained solution [Eqs. (6) and (7)] applied to the 24-h time series consistently overestimated measured $a_g(440)$ by an amount ranging from 0.18 to 0.55 m^{-1} [Fig. 6(b)]. The overestimation of $a_g(440)$ by the unconstrained solution was accompa-

Table 3. Statistical Comparison between Measured and Calculated Absorption Parameters

Parameter	Solution Procedure	Rhode River r^2	Rhode River rms Error[a]	Rhode River Mean Error	St. Johns River r^2	St. Johns River rms Error[a]	St. Johns River Mean Error
ϵ							
	Unconstrained[b]	0.995	0.004	**0.003**[c]	0.96	0.020	−0.005
	Statistically augmented[d]	0.94	0.015	**0.006**	0.97	0.016	**−0.012**
	Measurement constrained[e]	0.92	0.016	<0.001	0.98	0.016	**−0.012**
$a_g(440)$							
	Unconstrained[b]	0.02	0.31	0.05	0.60	1.74	0.75
	Statistically augmented[d]	0.41	0.22	**0.13**	0.84	1.21	0.31
$a_\phi(676)$							
	Unconstrained[b]	0.76	0.15	**−0.08**	0.85	0.07	−0.03
	Statistically augmented[d]	0.71	0.17	**−0.09**	0.57	0.14	−0.05
	Measurement constrained[e]	0.79	0.14	**−0.06**	0.01	0.29	**−0.15**
$a_{p-\phi}(440)$							
	Unconstrained[b]	0.65	0.42	0.05	0.00	1.14	−0.19
	Statistically augmented[d]	0.79	0.21	**−0.05**	0.46	0.26	−0.03
	Measurement constrained[e]	0.84	0.25	**0.13**	0.00	1.66	**0.85**

[a]Root-mean-square error between measured and calculated value.
[b]Equations (6) and (7).
[c]Boldface indicates statistically significant mean error ($P < 0.05$).
[d]Equations (9) and (10).
[e]Equation (11).

nied by underestimation of $a_\phi(676)$ [Fig. 6(c), filled squares] and of $a_{p-\phi}(440)$ [Fig. 6(d), filled squares]. Application of the statistically augmented procedure [Eqs. (8)–(10)] improved estimates for portions of the day, but large errors persisted at times of high water level from approximately 0400 to 1000 h and 1600 to 2000 h [Fig. 6(b)]. Moreover, these errors were correlated with changes in the scattering coefficient, indicating incorrect partitioning of short-term changes in absorption by dissolved and particulate fractions at those times [see Fig. 6(a), filled squares; Fig. 6(b) open circles]. The statistically augmented procedure improved the overall magnitude of estimates of both $a_\phi(676)$ [Fig. 6(c), open circles] and $a_{p-\phi}(440)$ [Fig. 6(d), open circles], but the short-term changes in measured $a_{p-\phi}(440)$ at the times noted above were not resolved. The measurement-constrained solution [Eq. (11) and hourly CDOM measurements] overestimated $a_\phi(676)$ prior to approximately 1400 h and produced good estimates in the later part of the day [Fig. 6(c), crosses]. Conversely, the measurement-constrained procedure produced good estimates of $a_{p-\phi}(440)$ prior to 1400 h and overestimated maximal measured values from 1700 to 1800 h [Fig. 6(d), crosses]. All estimates of $a_\phi(676)$ changed in parallel with measurements of chlorophyll [Fig. 6(c), open diamonds]. Finally, we note that application of the measurement-constrained procedure with the value fixed at the midday measurement (data not shown) gave estimates of $a_{p-\phi}(440)$ nearly identical with those determined with hourly measurements to constrain the procedure, which was due to the relative (to other components) constancy of CDOM absorption during this time period.

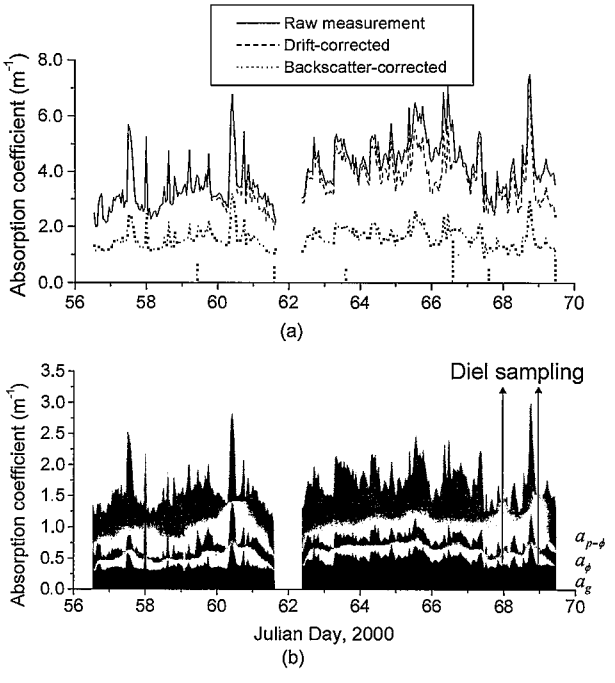

Fig. 5. Application of the unconstrained solution to a 15-day time series of continuously monitored data from the Rhode River, Maryland. (a) Absorption coefficient at 440 nm before and after correction for drift and backscatter. Vertical dotted curves indicate timing and magnitudes of drift corrections. (b) Estimates of components of $a_{t-w}(440)$ by factors indicated to the right of the graph.

6. Discussion

The matrix solution for the coefficients scaling the absorption by CDOM, phytoplankton, and nonpigmented particulate matter [Eqs. (5)–(7)] is a simple consequence of the linearity of inherent optical properties. We have shown that measurements of spectral absorption coefficients at four wavelengths are

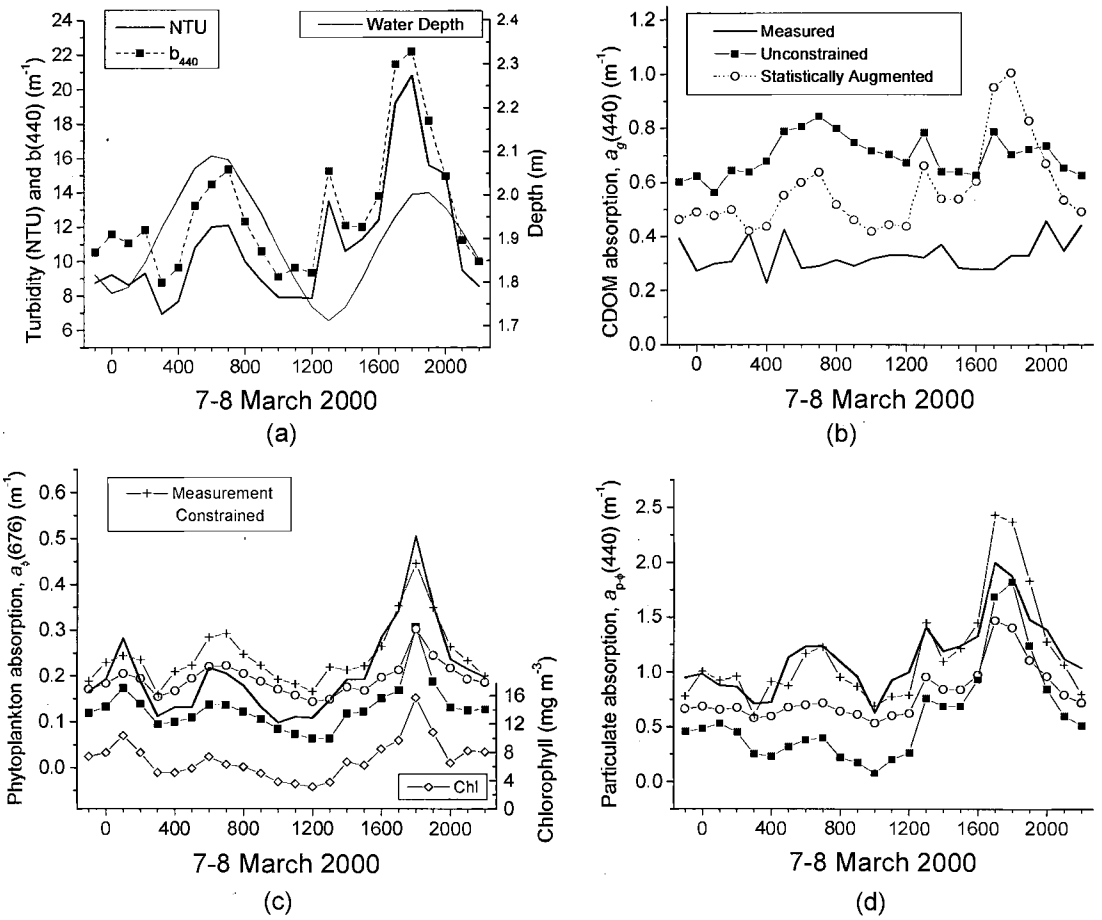

Fig. 6. Comparison of optical parameters estimated by the three solution procedures with water quality measurements made at hourly intervals 7–8 March 2000. (a) Turbidity, b(440), and depth; (b) measured and estimated a_g(440); (c) measured and estimated a_ϕ(676); (d) measured and estimated $a_{p-\phi}$(440). NTU, nephelometric turbidity units.

sufficient also to solve for the backscatter correction factor ϵ, which is specific to the ac-9 instrument. Even though the unconstrained solution for a_g(440) and $a_{p-\phi}$(440) may be sensitive to deviations from assumed spectral shapes leading to undesirable results like negative absorption coefficients [Fig. 4(d), filled squares], the errors in estimated a_g(440) and in $a_{p-\phi}$(440) were partially offsetting, allowing relatively precise estimation of ϵ and hence also of total absorption and scattering coefficients [Figs. 3(a) and 4(a)]. This is a significant advancement for case 2 waters where there may be measurable residual absorption by CDOM or nonpigmented particulates in the near infrared.[17,34] In such cases, use of the maximal ϵ that assumes $a_{t-w}(715) = 0$ would result in consistent underestimation of total absorption and overestimation of scattering coefficients at all other wavelengths. In our estimates the quantity $a_m(715)/b_m(715)$ consistently overestimates ϵ determined according to Eq. (6) by approximately 5%.

The solutions derived do not presuppose functional forms for normalized absorption spectra of the absorbing components, although assumption of a negative exponential for absorption by CDOM is convenient because the small absorbances at long wavelengths can be difficult to measure accurately without a long path-length spectrophotometer.[29] The normalized absorption spectra for the Rhode River and the St. Johns River appeared similar (Fig. 2), but the small differences observed were important to the overall performance of the solution procedures in the respective systems.

The normalized absorption spectra for nonpigmented particulate matter closely resembled negative exponential functions of wavelength, but appeared to decline more steeply from 650 to 715 nm than a true exponential (Fig. 2). Therefore we used tabulated values for $p(\lambda)$ rather than a mathematical function. Others have estimated spectral shapes for absorption by suspended mineral matter that increase at wavelengths from 600 to 750 nm.[32,33,35] The solution schemes of Eqs. (5)–(11) can accommodate such spectral shapes wherever warranted by the observations. It may be that adsorption of organic matter to the surface of minerals may mask any absorption features unique to suspended minerals in coastal regions draining forested and farmed watersheds (e.g., the Rhode River) or wetlands (St. Johns River). Absent a distinguishing spectral absorption feature, we see little prospect for further partitioning

of $a_{p-\phi}$ into separate mineral and organic detrital fractions.

The site-specific, statistically augmented modifications increased the accuracy of the solution by constraining the value of the absorption-to-scattering ratio at 440 nm, ρ, to vary within observed limits, or as in the St. Johns River, to a constant mean value. A single value was sufficient in the St. Johns River because of the extreme dominance of variation in absorption by CDOM [Fig. 4(b)]. In contrast, in the Rhode River where absorption by CDOM and nonpigmented particulates were of similar magnitude [Figs. 3(b) and 3(d)], it was necessary to employ a regression that recovered at least some of the variability in ρ. The regression utilizes only data that are measured by the ac-9, and the principal components upon which it is based seem to be consistent with meaningful properties of the particulate matter in the system. The drawback with a site-specific statistical approach is that it is always possible to encounter a combination of factors outside the domain of observations used in development of the regression, which might lead to the procedure yielding unreasonable values, e.g., calculated $\rho < 0$. Similarly, fine-scale variations may not be well resolved, as was the case in the diel study [Fig. 6(d)].

In some systems, other ancillary data can be used to reduce uncertainty in the normalized absorption functions. For example, Roesler *et al.*[10] used measurements of the phaeophytin-to-chlorophyll ratio to improve their prediction of the ratio of $a_\phi(436)$: $a_\phi(676)$, which in our notation is $\phi(436)$ (although 436 nm is not a standard ac-9 wavelength). Similarly, Bricaud *et al.*[31] found that a power-law function of chlorophyll explained much of the variability in chlorophyll-specific absorption by phytoplankton in a range of ocean waters. The same relationship can be transformed to express $\phi(\lambda)$ as a function of $a_\phi(676)$. Use of such information transforms the problem into a nonlinear system and requires iterative calculations for the solution. Neither of these relationships were found to provide better predictions of $\phi(\lambda)$ than the mean in the two estuaries examined here.

Application of the solutions to continuously monitored data in the Rhode River demonstrated substantial short-term variability in optical properties, generally attributed to changes in nonpigmented particulate absorption, often correlated with changes in a_ϕ [Figs. 5(b)–5(d)]. Diel hourly water sampling and laboratory determination of optical properties demonstrated conclusively that the calculated variations were indeed associated with changes in water quality parameters (Fig. 6). Furthermore, absorption by nonpigmented particulates estimated with the measurement-constrained procedure agreed well quantitatively with major changes in measurements made with the filter pad technique [Fig. 6(d)]. The tendency of the statistically augmented procedure to attribute short-term variations in particulate absorption to variations in CDOM indicates that short-term advective changes in the absorption-to-scattering ratio ρ were not well resolved by the statistical relationship derived from samples collected over a full annual cycle. Estimation of separate empirical statistical models for shorter segments of data might improve the estimates, but that then defeats our purpose of using the statistically augmented procedure, which is to avoid the necessity of making temporally intensive measurements.

Absorption by nonpigmented particulates quantitatively dominated total absorption at 440 nm in the Rhode River during a 15-day period in March 2000 [Fig. 5(b)]. These measurements were made prior to the spring phytoplankton bloom in this system.[36] More complete seasonal measurements will be needed to fully assess the relative importance of the three absorption components to determine the underwater light climate in the system.

7. Conclusions

Comparing results from the Rhode River with those from the St. Johns River in which absorption was dominated by CDOM, we reach the general conclusion that a_ϕ is well resolved in either system because of its characteristic peak at 676 nm. After that, the largest absorption component is also well resolved [see Figs. 3(d) and 4(b)], but the relatively minor component, whether a_g (i.e., Rhode River) or $a_{p-\phi}$ (St. Johns River), is less precisely determined, but largely accurate in the overall mean when used with large amounts of data typically collected in monitoring or mapping applications.

The capability to distinguish the components of absorption has considerable potential to focus management efforts in optically deteriorated waters. The Rhode River once supported submerged vascular plants, but populations disappeared in the late 1960s.[37] Continuous monitoring of absorption and attenuation coefficients during March 2000 indicated that nonalgal particulates dominated absorption [Fig. 5(b)], but absorption and attenuation coefficients measured later during the spring bloom were much higher and were dominated initially by chlorophyll and then by detritus.[38] This shift, which would not have been detected by measurements of chlorophyll alone, extended the impact of the bloom on optical properties by an additional two weeks. Partitioning of absorption components thus indicates that we could lower absorption by both chlorophyll and by detritus by addressing the eutrophication problem.

Although our research described in this paper has been funded in part by the Coastal Intensive Site Network program of the U.S. Environmental Protection Agency through grant R826943-01-0, it has not been subjected to the Agency's required peer and policy review and therefore does not necessarily reflect the views of the Agency and no official endorsement should be inferred. Research on the St. Johns River was funded by St. Johns River Water Management District under contract 99B144B to C. L. Gallegos. We thank K. Yee and D. Sparks for assistance in the

field and laboratory and J. Messer, M. Burns, and A. McKinney for field assistance at the St. Johns River. C. Roesler and M. Dowell and an anonymous reviewer provided helpful comments on a previous draft.

References

1. T. Platt and S. Sathyendranath, "Oceanic primary production: estimation by remote sensing at local and regional scales," Science **241,** 1613–1620 (1988).
2. M. J. Behrenfeld, J. T. Randerson, C. R. McClain, G. C. Feldman, S. O. Los, C. J. Tucker, P. G. Falkowski, C. B. Field, R. Frouin, W. E. Esaias, D. D. Kolber, and N. H. Pollack, "Biospheric primary production during an ENSO transition," Science **291,** 2594–2597 (2001).
3. H. R. Gordon and A. Y. Morel, *Remote Assessment of Ocean Color for Interpretation of Satellite Visible Imagery. A Review* (Springer-Verlag, New York, 1983).
4. C. D. Mobley, *Light and Water. Radiative Transfer in Natural Waters* (Academic, New York, 1994).
5. W. C. Dennison, R. J. Orth, K. A. Moore, J. C. Stevenson, V. Carter, S. Kollar, P. W. Bergstrom, and R. A. Batiuk, "Assessing water quality with submersed aquatic vegetation," BioScience **43,** 86–94 (1993).
6. C. L. Gallegos, "Calculating optical water quality targets to restore and protect submersed aquatic vegetation: overcoming problems in partitioning the diffuse attenuation coefficient for photosynthetically active radiation," Estuaries **24,** 381–397 (2001).
7. T. Dickey, D. Frye, H. Jannasch, E. Boyle, D. Manov, D. Sigurdson, J. McNeil, M. Stramska, A. Michaels, N. Nelson, D. Siegel, G. Chang, J. Wu, and A. Knap, "Initial results from the Bermuda testbed mooring program," Deep-Sea Res. I **45,** 771–794 (1998).
8. G. C. Chang and T. D. Dickey, "Partitioning *in situ* total spectral absorption by use of moored spectral absorption–attenuation meters," Appl. Opt. **38,** 3876–3887 (1999).
9. H. Claustre, F. Fell, K. Oubelkheir, L. Prieur, A. Sciandra, B. Gentili, and M. Babin, "Continuous monitoring of surface optical properties across a geostrophic front: biogeochemical inferences," Limnol. Oceanogr. **45,** 309–321 (2000).
10. C. S. Roesler, M. J. Perry, and K. L. Carder, "Modeling in situ phytoplankton absorption from total absorption spectra in productive inland marine waters," Limnol. Oceanogr. **34,** 1510–1523 (1989).
11. R. W. Preisendorfer, *Hydrologic Optics* (National Oceanic and Atmospheric Administration, Washington, D.C., 1976).
12. A. Morel, "In-water and remote measurements of ocean color," Boundary-Layer Meteorol. **18,** 177–201 (1980).
13. J. T. O. Kirk, "Monte Carlo modeling of the performance of a reflective tube absorption meter," Appl. Opt. **31,** 6463–6468 (1992).
14. J. R. V. Zaneveld, J. C. Kitchen, and C. Moore, "The scattering error correction of reflecting-tube absorption meters," in *Ocean Optics XII*, J. S. Jaffe, ed., Proc. SPIE **2258,** 44–55 (1994).
15. C. S. Roesler, "Theoretical and experimental approaches to improve the accuracy of particulate absorption coefficients derived from the quantitative filter technique," Limnol. Oceanogr. **43,** 1649–1660 (1998).
16. J. T. O. Kirk, *Light and Photosynthesis in Aquatic Ecosystems* (Cambridge U. Press, Cambridge, UK, 1994).
17. H. Hakvoort and R. Doerffer, "Estimation of specific absorption coefficients of turbid coastal water constituents using the AC-9 and asymptotic attenuation coefficients," in *Ocean Optics XIII*, S. G. Ackleson, ed., SPIE **2963,** 435–439 (1997).
18. H. Maske and H. Haardt, "Quantitative in vivo absorption spectra of phytoplankton: detrital absorption and comparison with fluorescence excitation spectra," Limnol. Oceanogr. **32,** 620–633 (1987).
19. A. Bricaud and D. Stramski, "Spectral absorption coefficients of living phytoplankton and nonalgal biogenous matter: a comparison between the Peru upwelling area and the Sargasso Sea," Limnol. Oceanogr. **35,** 562–582 (1990).
20. C. L. Gallegos, D. L. Correll, and J. W. Pierce, "Modeling spectral diffuse attenuation, absorption, and scattering coefficients in a turbid estuary," Limnol. Oceanogr. **35,** 1486–1502 (1990).
21. H. R. Gordon, "Can the Lambert-Beer law be applied to the diffuse attenuation coefficient of ocean water?," Limnol. Oceanogr. **34,** 1389–1409 (1989).
22. T. E. Jordan, D. L. Correll, J. Miklas, and D. E. Weller, "Long-term trends in estuarine nutrients and chlorophyll, and short-term effects of variation in watershed discharge," Mar. Ecol. Prog. Ser. **75,** 121–132 (1991).
23. C. L. Gallegos and T. E. Jordan, "Seasonal progression of factors limiting phytoplankton pigment biomass in the Rhode River estuary, Maryland (USA). II. Modeling N versus P limitation," Mar. Ecol. Prog. Ser. **161,** 199–212 (1997).
24. T. E. Jordan, D. L. Correll, J. Miklas, and D. E. Weller, "Nutrients and chlorophyll at the interface of a watershed and an estuary," Limnol. Oceanogr. **36,** 251–267 (1991).
25. F. W. I. Morris, "Volume 3 of the lower St. Johns River basin reconnaissance: hydrodynamics and salinity of surface water" Tech. Rep. SJ95–9 (St. Johns River Water Management District, Palatka, Florida, 1995).
26. M. Kishino, M. Takahashi, N. Okami, and S. Ichimura, "Estimation of the spectral absorption coefficients of phytoplankton in the sea," Bull. Mar. Sci. **37,** 634–642 (1985).
27. S. W. Jeffrey and G. F. Humphrey, "New spectrophotometric equations for determining chlorophyll a, b, $c1$, and $c2$ in higher plants, algae and natural phytoplankton," Biochem. Physiol. Pflanz. **167,** 191–194 (1975).
28. A. Bricaud, A. Morel, and L. Prieur, "Optical efficiency factors of some phytoplankters," Limnol. Oceanogr. **28,** 816–832 (1983).
29. L. Prieur and S. Sathyendranath, "An optical classification of coastal and oceanic waters based on the specific spectral absorption curves of phytoplankton pigments, dissolved organic matter, and other particulate materials," Limnol. Oceanogr. **26,** 671–689 (1981).
30. K. L. Carder, R. G. Steward, G. R. Harvey, and P. B. Ortner, "Marine humic and fulvic acids: their effects on remote sensing of ocean chlorophyll," Limnol. Oceanogr. **34,** 68–81 (1989).
31. A. Bricaud, M. Babin, A. Morel, and H. Claustre, "Variability in the chlorophyll-specific absorption coefficients of natural phytoplankton: analysis and parameterization," J. Geophys. Res. **100,** 13321–13332 (1995).
32. R. P. Bukata, J. H. Jerome, K. Y. Kondratyev, and D. V. Pozdnyakov, "Estimation of organic and inorganic matter in inland waters: optical cross sections of Lakes Ontario and Ladoga," J. Great Lakes Res. **17,** 461–469 (1991).
33. E. A. Gallie and P. A. Murtha, "Specific absorption and backscattering spectra for suspended minerals and chlorophyll-a in Chilko Lake, British Columbia," Remote Sens. Environ. **39,** 103–118 (1992).
34. G. M. Ferrari, N. Hoepffner, and M. Mingazzini, "Optical properties of the water in a deltaic environment: prospective tool to analyze satellite data in turbid waters," Remote Sens. Environ. **58,** 69–80 (1996).
35. A. Morel and A. Bricaud, "Theoretical results concerning light

absorption in a discrete medium, and application to specific absorption of phytoplankton," Deep-Sea Res. **28,** 1375–1393 (1981).
36. C. L. Gallegos, T. E. Jordan, and D. E. Correll, "Interannual variability in spring bloom timing and magnitude in the Rhode River, Maryland (USA): observations and modeling," Mar. Ecol. Prog. Ser. **154,** 27–40 (1997).
37. C. H. Southwick and F. W. Pine, "Abundance of submerged vascular vegetation in the Rhode River from 1966 to 1973," Chesapeake Sci. **16,** 147–151 (1975).
38. C. L. Gallegos and T. E. Jordan, "Impact of the Spring 2000 phytoplankton bloom in Chesapeake Bay on optical properties and light penetration in the Rhode River, Maryland," Estuaries, accepted for publication.